THE JOURNAL OF PHYSICAL CHEMISTRY A

ARTICLE

pubs.acs.org/JPCA

Large Shift and Small Broadening of Br_2 Valence Band upon Dimer Formation with H_2O: An Ab Initio Study

Ricardo Franklin-Mergarejo

Instituto Superior de Tecnologías y Ciencias Aplicadas, Ave. Salvador Allende y Luaces, Quinta de los Molinos, Plaza, Habana 10600, Aptdo. Postal 6163, Ciudad Habana, Cuba

Université de Toulouse, UPS, Laboratoire Collisions Agrégats Réactivité, IRSAMC, F-31062 Toulouse, France

CNRS, UMR 5589, F-31062 Toulouse, France

Jesus Rubayo-Soneira

Instituto Superior de Tecnologías y Ciencias Aplicadas, Ave. Salvador Allende y Luaces, Quinta de los Molinos, Plaza, Habana 10600, Aptdo. Postal 6163, Ciudad Habana, Cuba

Nadine Halberstadt*

Université de Toulouse, UPS, Laboratoire Collisions Agrégats Réactivité, IRSAMC, F-31062 Toulouse, France

CNRS, UMR 5589, F-31062 Toulouse, France

Tahra Ayed†

Centro de Investigaciones Químicas, UAEM, Cuernavaca, Mor. 62209, México

Margarita I. Bernal-Uruchurtu and Ramón Hernández-Lamoneda

Centro de Investigaciones Químicas, UAEM, Cuernavaca, Mor. 62209, México

Kenneth C. Janda

Department of Chemistry, University of California, Irvine, California 92697-2025, United States

ABSTRACT: Valence electronic excitation spectra are calculated for the $H_2O\cdots Br_2$ complex using highly correlated ab initio potentials for both the ground and the valence electronic excited states and a 2-D approximation for vibrational motion. Due to the strong interaction between the O−Br and the Br−Br stretching motions, inclusion of these vibrations is the minimum necessary for the spectrum calculation. A basis set calculation is performed to determine the vibrational wave functions for the ground electronic state and a wave packet simulation is conducted for the nuclear dynamics on the excited state surfaces. The effects of both the spin−orbit interaction and temperature on the spectra are explored. The interaction of Br_2 with a single water molecule induces nearly as large a shift in the spectrum as is observed for an aqueous solution. In contrast, complex formation has a remarkably small effect on the $T = 0$ K width of the valence bands due to the fast dissociation of the dihalogen bond upon excitation. We therefore conclude that the widths of the spectra in aqueous solution are mostly due to inhomogeneous broadening.

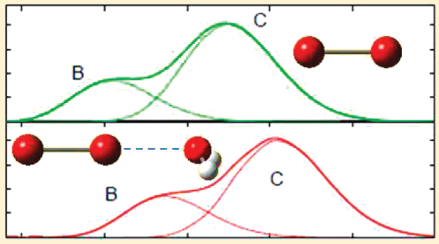

I. INTRODUCTION

The large solvent shifts for the valence excitation spectra of halogen molecules have been studied for over a century.[1,2] For a considerable portion of that time, it seemed that these solvent shifts would soon be explained by fairly simple models, but no self-consistent model was ever found. Recently both the valence electronic excitation spectra and the Raman spectra of bromine in several aqueous environments have been reexamined.[3−5] The maxima of both the $B(^3\Pi_{0_u^+}) \leftarrow X(^1\Sigma_g^+)$ and the $C(^1\Pi_{1_u}) \leftarrow X(^1\Sigma_g^+)$ bands shift about 1750 cm^{-1} to the

Special Issue: Victoria Buch Memorial

Received: October 30, 2010
Revised: December 23, 2010
Published: February 01, 2011

blue in going from the gas phase to liquid aqueous solution while the $^{79}Br-^{81}Br$ stretching frequency shifts from 323 to 306 cm^{-1}. These large frequency shifts are indicative of a strong $H_2O\cdots Br_2$ interaction, yet bromine is only slightly soluble in water. In contrast to liquid solution, bromine is quite soluble in solid aqueous solution and forms a clathrate hydrate solid that is stable up to 5.5 °C. In clathrate hydrate solids the water molecules form cages, some of which are occupied by bromine molecules. The existence of such solids has been known for two centuries,[6,7] but the most common bromine clathrate hydrate crystal structure was only elucidated in 1997.[8] A total of 80% of the bromine molecules in this crystal are trapped in 24 water molecule cages referred to as $5^{12}6^2$ cages because they contain two hexagonal faces on top and bottom and a ring of 12 pentagonal cages forming the sides. The long diameter of these cages is 8.7 Å. Taking the oxygen atom radius to be 1.52 Å, the bromine atom radius to be 1.85 Å and the ground state bromine bond length to be 2.28 Å, giving an O−Br−Br−O length of 9.02 Å, it might be expected that the bromine fits quite tightly in these cages. The blue shift of the bromine valence electronic spectrum from the gas phase to the clathrate hydrate crystal is 880 cm^{-1}, only half that of liquid aqueous solution. The $^{79}Br-^{81}Br$ stretching frequency in the cages is 321 cm^{-1}, which is much closer to that of the gas phase than that of liquid aqueous solution. So, in spite of the close Br−O contact in the bromine hydrate crystals, the shift of the valence spectrum is half that of aqueous solution and the vibrational frequency is only slightly shifted from that of the gas phase.

The spectra of bromine can also be studied in crystals in which the bromine is contained in slightly larger, more nearly spherical, $5^{12}6^4$ cages, with 9.6 Å diameter. In these cages, the valence electronic spectrum shift is down to 440 cm^{-1} and the Raman frequency is 318 cm^{-1}. So, the electronic spectrum shift is smaller in the larger cages than in the smaller $5^{12}6^2$ cages but the vibrational frequency shift is somewhat larger. We speculate that the larger cages perturb the bromine electronic excited states less strongly than the smaller cages, and that in the ground state the attractive forces to the cage walls dominate except for the smaller $5^{12}6^2$ cages where the attractive and repulsive forces on the bromine bond approximately cancel. The $5^{12}6^2$ cage was found by Schofield and Jordan[9] to have the smallest stability of the three cage types in which Br_2 can fit ($5^{12}6^2$, $5^{12}6^3$, $5^{12}6^4$), and this difference will certainly increase if Br_2 is in a vibrationally excited state. A long-term goal of the types of calculations presented in this paper is to understand this data in more detail.

Modeling the spectra of bromine in either liquid or solid aqueous solution is difficult because the interaction is both strong and very anisotropic. In the halogen bond configuration, $H_2O-Br-Br$, the O−Br−Br configuration is linear and the O−Br bond is unusually short, $R_e(O-Br) = 2.797$ Å, and strong, $D_e = 1182$ cm^{-1},[10] compared to usual van der Waals interactions. In contrast, for the next lowest potential minimum, the Br−H coordinated conformer, in which one hydrogen of the water molecule interacts with the halogen π^* HOMO, $D_e = 600$ cm^{-1}.[11] Also, the valence excited state potentials are quite different from those of the ground state. The symmetry of the Br_2 excitation is $\sigma^* \leftarrow \pi^*$, so upon excitation some electron density moves from the cylinder around the Br−Br bond to the ends of the molecule. Thus, Franck−Condon excitation results in a repulsive O−Br interaction in the excited state. The strong O−Br bond in the ground electronic state and the repulsive O−Br interaction in the excited electronic states qualitatively explain the strong blue shift in liquid aqueous solution.

Unfortunately, a full simulation of the spectra will be extremely complicated. Even for the $H_2O\cdots Br_2$ dimer there are nine vibrational modes that need to be included for a full calculation. Thus, reduced dimensionality calculations are necessary to gain initial insight into important effects on the spectra, while more complete work is in progress. In this paper, we present a two-dimensional calculation of the valence electronic excitation spectrum of the $H_2O\cdots Br_2$ dimer as a first step along this path. This is the minimum dimensionality that includes the essential features of the spectra: both the Br−Br and the O−Br coordinates become unbound in the Franck−Condon region of the valence electronic excitation. The potential energy surfaces for the spectrum calculations are obtained from high level ab initio electronic structure calculations,[10] to which we add spin−orbit interaction. Two-dimensional vibrational wave functions are then calculated for the electronic ground state surface of the dimer. Excitation spectra are calculated using a wave packet description of the nuclear motion in the valence excited states.

The importance of several effects and approximations are tested. Calculations have been performed with and without spin−orbit coupling and at three different temperatures. The spectator model for the spectra is also investigated. Although the water molecule shifts the spectrum of the bromine chromophore quite substantially, it has little effect on the width of the spectrum at 0 K. This means that treating the water molecule as a spectator is a surprisingly good approximation. In turn, this gives us hope that more complete simulations of the spectra for the condensed phase systems may be feasible in the not-too-distant future.

II. METHOD

We have used a two-dimensional model to determine the $H_2O\cdots Br_2$ absorption spectra. One dimension is the chromophore intramolecular coordinate, the Br···Br distance r, and since the O−Br coordinate becomes dissociative in the excited states, the intermolecular center of mass distance R is also essential to obtain a reasonable approximation to the full spectrum. The other coordinates are frozen at their value in the equilibrium configuration of $H_2O\cdots Br_2$ determined in ref 10. At equilibrium, the O, Br, and Br atoms are aligned, and the hydrogen atoms symmetrically bent off the O−Br−Br axis, the water C_{2v} axis being tilted by 49°.

A. Potential Energy Surfaces Including Spin−Orbit Effects. A detailed study of the spectroscopic properties of the bromine molecule must include spin−orbit effects. From a qualitative point of view their inclusion is crucial to obtain the relevant spin−orbit states ($A^3\Pi_{1_u}$, $B^3\Pi_{0_u^+}$, $C^1\Pi_{1_u}$) from their purely electronic main components and also to properly reproduce their corresponding dissociation limits. The quantitative calculation of other system properties, such as electronic excitation energies, also depends on their inclusion. Of particular interest to us are the possible intermolecular effects on the spin−orbit interactions. The methodology we have followed has been described in detail in a related study of the $Ne\cdots Cl_2$ system[12] where the spin−orbit effects also play a significant role. They were also included in our previous study of the $H_2O\cdots Cl_2$ dimer, and their influence on the spectrum was found to be moderate, due to the smaller spin−orbit splitting of Cl (882.35 cm^{-1})[13] and also to a weaker intermolecular interaction. We expect more important influence on the $H_2O\cdots Br_2$ spectra because of the larger spin−orbit splitting for Br (3685.23 cm^{-1})[14] as well as a stronger bromine water interaction.

Here we summarize the main ingredients. We use the relativistic effective core potential (RECP) of bromine (ECP28MWB_VQZ) developed by the Stuttgart group[15,16] which provides an efficient way for including spin−orbit effects. The original valence basis set has been extended with polarization and diffuse functions to yield the final set *5s5p4d3f2g*. The extra basis functions consist of diffuse *d*, *f*, and *g* functions with exponents 0.1230, 0.1822, and 0.3196, respectively. For the water molecule we use the AVTZ (augmented correlation consistent triple-ζ) basis set. The relevant spin−orbit states are obtained by diagonalizing the total Hamiltonian, which consists of the usual electronic term plus the spin−orbit interaction term. The basis set for diagonalization is obtained by first optimizing the orbitals in a complete active space (CAS) defined by the valence electrons and orbitals of bromine together with a state-averaging of nine electronic states close in energy to the states involved in the spectroscopy. We then perform multireference configuration interaction (MRCI) calculations to include dynamic electron correlation including the valence electrons of the water molecule. The total number of spin−orbit states obtained is 36. All calculations were performed with the MOLPRO2006.1 package.[17]

The final potential energy surfaces are constructed by adding the spin−orbit correction obtained in the calculations described above to the highly correlated but purely electronic energies obtained in ref 10 (Note that the A' symmetry of the *B* and *C* electronic states in ref 10 loses its meaning when spin−orbit correction is included).

B. Transition Dipole Moment. The transition dipole moment surface for the dipole-allowed transition between the ground and singlet excited state was taken from ref 10. Although its value varies with both *r* and *R*, the resulting effect of these dependences on the spectra is not very important because the variation is modest in the Franck−Condon region of the valence excitation.

C. Principle of the Absorption Spectrum Calculation (*T* = 0, 120, and 300 K). The dynamical method has been described in a previous publication.[18] Briefly, the bound states $\Phi_{Xn}(r,R)$ in the X electronic surface are determined by diagonalizing the Hamiltonian matrix in a direct product DVR basis set (15, 60 wave functions obtained by diagonalizing the *r*,*R* operator in a harmonic oscillator basis set with r_e = 2.325 Å, R_e = 4.086 Å and $\hbar\omega_r$ = 314.4 cm^{-1}, $\hbar\omega_R$ = 96.9 cm^{-1}, respectively). The atomic masses for ^{79}Br, H, and ^{16}O were taken from NIST.[19]

The *T* = 0 K absorption spectrum is given by the Fourier transform of the autocorrelation function of a wave packet propagating on the excited state surface. This wave packet is initially determined as the bound state wave function (determined in the previous step) multiplied by the transition dipole moment. We used the split-operator propagation technique with time steps of 0.1 au. The grid in *r* had 256 points from 2.10 to 2.90 Å, and the one in *R* had 256 points from 3.4 to 16 Å.

To study the effect of temperature on the absorption spectra, we have summed the spectra from each individual excited vibrational state of Br_2 or $H_2O\cdots Br_2$ multiplied by its Boltzmann factor at the chosen temperature (*T* = 120 and 300 K). As in ref 20, we have simplified the sum over rotational levels. We have used one value of the rotational angular momentum $\overline{J}$ defined by

$$Q_R = (2\overline{J}+1)e^{-B\overline{J}(\overline{J}+1)/k_BT} \quad (1)$$

where Q_R is the rotational partition function, *B* is the rotational constant of the molecule assumed to be the same for all vibrational levels, and k_B is the Boltzmann constant. The resulting values are $\overline{J}$ (*T* = 120 *K*) = 29 for Br_2 and 43 for $H_2O\cdots Br_2$, and $\overline{J}$ (*T* = 300 K) = 45 for Br_2 and 70 for $H_2O\cdots Br_2$.

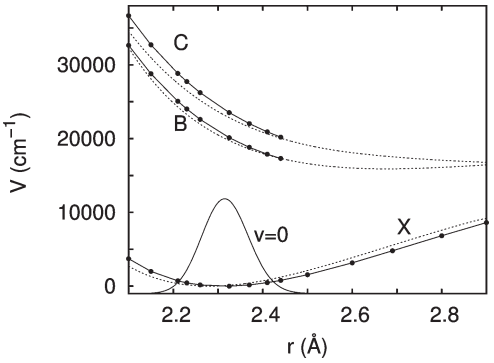

Figure 1. Computed Br_2 curves including spin−orbit coupling (straight lines with dots), compared to empirical curves from refs 21−25 (dashed lines). The *v* = 0 wave function shows the Franck−Condon region.

D. Spectator Model. Finally, we have also tested the spectator model introduced in ref 18. In this model the water molecule does not have time to move during the halogen dissociation, but its presence alters the Br−Br potential energy curves.

III. RESULTS

In Figure 1, we show the calculated Br_2 curves for the *X*, *B*, and *C* states, including spin−orbit coupling, along with the empirical curves[21−25] that were fitted to reproduce the experimental Br_2 valence absorption spectra. The comparison shows that the methods employed here are quite good for determining the potential energy curves of the free Br_2 molecule. The ab initio curves are slightly more repulsive than the empirical ones in the inner part of the Franck−Condon region for all three states. The *X* state potential is slightly too attractive at long-range. Because the region of repulsion is different for the ground and valence excited states, these differences have important effects on the calculated spectra, as will be discussed in more detail below.

A. Effect of Spin−Orbit Interaction on the Potential Energy Surfaces. The spin−orbit corrections ΔE^{SOC} to the *B* and *C* states of $H_2O\cdots Br_2$ are shown in Figure 2. As can be seen from this figure, they depend on both the intra- (*r*) and inter- (*R*) molecular coordinates. The most important point for the spectrum calculation is that in the Franck−Condon region (2.10 Å ≤ *r* ≤ 2.44 Å, 3.8 Å ≤ *R* ≤ 4.4 Å), the *B* state is shifted to higher energies by about one-third of the bromine atomic spin−orbit splitting (3685.23 cm^{-1}).[14] As noted in section IIA, this is essential for obtaining the correct relative energies of the *B* and *C* states. The corresponding shift of the *B* state curve of the isolated Br_2 molecule varies from 1293 to 1329 cm^{-1} for *r* = 2.44−2.10 Å. For H_2O-Br_2 distances larger than *R* = 3.5 Å, slightly shorter than the *B* state potential energy minimum distance, the effect of spin−orbit coupling on the H_2O-Br_2 interaction energy (variation of ΔE^{SOC} with *R*) is modest, less than 190 cm^{-1}. As the H_2O-Br_2 distance becomes smaller, in the region of the inner turning point, there is a stronger quenching of the spin−orbit interaction, but the slope along the *r* coordinate is only slightly affected.

The *C* state curve is also shifted to higher energies in the Franck−Condon region, although by a small amount. The corresponding shift of the isolated Br_2 molecule varies from −35 to 152 cm^{-1} for *r* = 2.44−2.10 Å, which is a more important

dx.doi.org/10.1021/jp110389z |*J. Phys. Chem. A* 2011, 115, 5983–5991

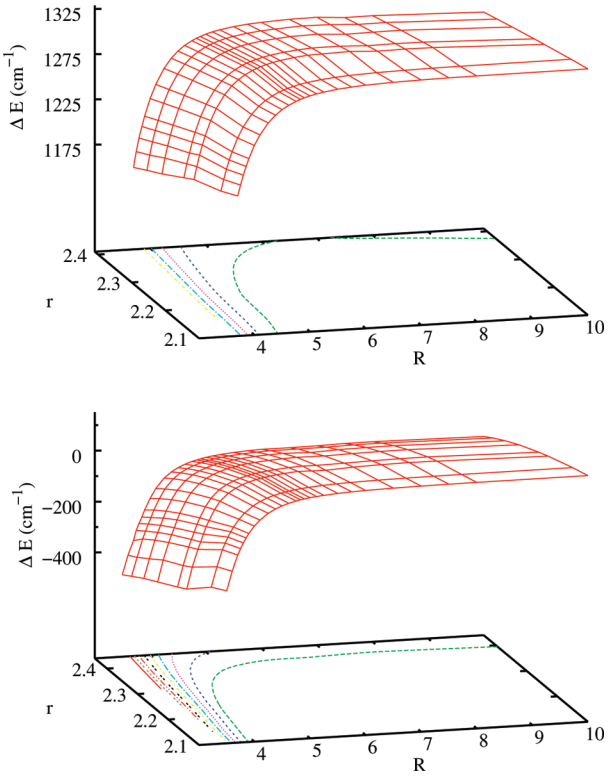

Figure 2. Spin−orbit correction for state B (top) and C (bottom): $\Delta E^{SOC}(r,R) = V^{SOC}(r,R) - V(r,R)$, where V^{SOC} represents the potential including spin−orbit coupling and V without.

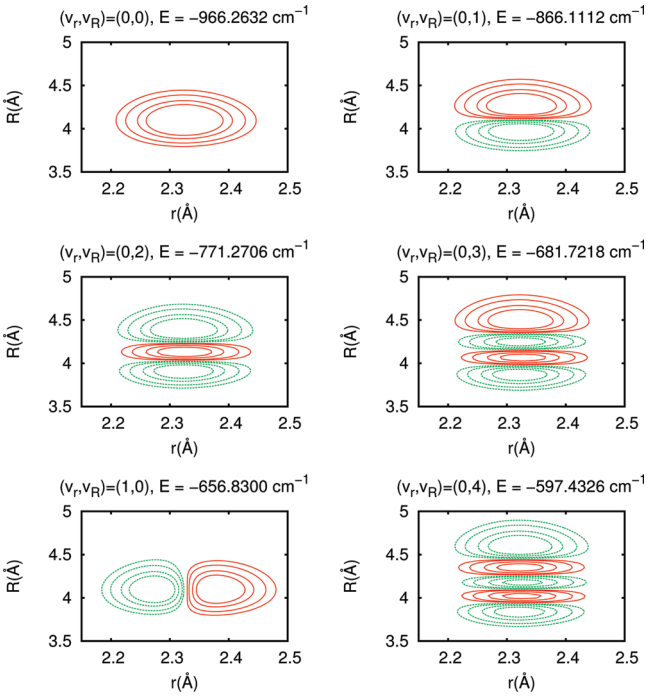

Figure 3. Six lowest energy $H_2O\cdots Br_2$ bound state wave functions: r is the Br−Br interatomic distance and R is the H_2O to Br_2 center of mass distance. Note that there are three weak bond excited states lower in energy than that of the first Br_2 stretching excited state. Also, note that there is little mixing between the coordinates evident in the shapes of the contours.

variation than for the B state. Interestingly the intermolecular effects are also larger than for the B state and this has consequences for the electronic shift in the spectra as will be discussed in section IIID.

B. $H_2O\cdots Br_2$ Bound States. The six lowest energy $H_2O\cdots Br_2$ 2-D ground electronic state bound vibrational state wave functions are shown in Figure 3, and some of their properties are given and compared to those of Br_2 in Tables 1 and 2. As might have been expected, the stretching amplitude along the weak bond coordinate is about 4 times that of the Br−Br stretch for the ground vibrational state. There are three weak-bond excited stretching states lower in energy than the first Br_2 stretching excited state. For the weak bond excited states closest in energy to the first Br_2 stretching state, the stretching amplitude has increased considerably, mainly for large R. This will be important for understanding the effect of temperature on the calculated spectra. That the two coordinates are not very mixed in this energy range is evident from the fact that the outer turning points for each coordinate change only slightly as the other coordinate is excited, and the node pattern is clearly assignable.

The data in Table 2 is useful for understanding the effect of dimer formation on the Br_2 bond. The E_0 values are relative to the bottom of the Br−Br potential in the absence of H_2O. $\hbar\omega$ and $\hbar\omega\chi$ values are obtained by fitting the energies in Table 1 to

$$\begin{aligned} E_{v_r, v_R} = & -D_e + \hbar\omega_r(v_r + 1/2) + \hbar\omega_R(v_R + 1/2) \\ & - \hbar\omega_r\chi_r(v_r+1/2)^2 - \hbar\omega_R\chi_R(v_R+1/2)^2 \\ & - \hbar(\omega\chi)_{rR}(v_r + 1/2)(v_R + 1/2) \end{aligned} \quad (2)$$

Table 1. Ab Initio Bound State Energies for the X Electronic State of $^{79}Br_2$ and of the $H_2O\cdots{}^{79}Br_2$ Complex

v_r / v_R	0	1	2
0	−966.2632(4)	−656.8300(4)	−349.3825(4)
1	−866.11124(7)	−556.39869(6)	−248.67493(5)
2	−771.2706(6)	−461.3263(6)	−153.365(1)
3	−681.7218(8)	−371.15(4)	
4	−597.4326(2)	−286.88(4)	
5	−518.335(2)	−206.7(2)	
6	−444.36(2)		
7	−375.9(4)		
8	−312.(3)		
9	−253.(15)		
10	−196.(36)		

The D_e value obtained in this calculation, 1184.3 cm^{-1}, is within 0.2 cm^{-1} of that calculated directly from the potential energy surface. r_0 and R_0 are calculated from $\langle 1/r^2\rangle$ and $\langle 1/R^2\rangle$, respectively, for the average over the ground state wave function. The r_0 value increases slightly, from 2.315 to 2.324 Å, and the $\hbar\omega_r$ value decreases slightly, from 317 to 311 cm^{-1}, upon dimer formation. These changes are due to halogen bond formation in which the water lone pair orbitals contribute some electron density to the bromine σ^* orbital. Since the X state is calculated to be slightly too attractive at long-range and too repulsive at short-range, the resulting r_0 value is 0.03 Å too long. The long-range

dx.doi.org/10.1021/jp110389z |J. Phys. Chem. A 2011, 115, 5983–5991

Table 2. Ab Initio Bound State Results for the *X* Electronic State of $^{79}Br_2$ and of the $H_2O\cdots{}^{79}Br_2$ Complex, Compared to Experimental Spectroscopic Data

	Br_2 calcd	$H_2O\cdots Br_2$ calcd	Br_2 expt	$H_2O\cdots Br_2$ expt	Br_2 in Ar matrix
E_0 (cm^{-1})	158.4209	−966.263			
r_0 (Å)	2.3149	2.324	2.283 26[a]	(2.283 26)[b]	
R_0 (Å)		4.097		4.4163[c]	
$\hbar\omega_r$ (cm^{-1})	317.374	311.279	325.314[d]	309.1−314.3[e]	318.65[f]
$\hbar\omega_r\chi_r$ (cm^{-1})	1.024	0.993	1.0787		0.820[f]
$\hbar\omega_R$ (cm^{-1})		105.323		101.4(10)[g]	
$\hbar\omega_R\chi_R$ (cm^{-1})		2.656			
$\hbar(\omega\chi)_{rR}$ (cm^{-1})		−0.279			

[a] Ref 21. [b] Fixed to the monomer value to deduce R_0, ref 31. [c] From $\langle R_{OBr}\rangle$ = 2:8506 Å in ref 31. [d] Ref 22. [e] For $H_2O\cdots Br_2$ in an argon matrix, ref 32. [f] Ref 33. [g] From k_σ = 9.8(2) Nm^{-1} in ref 31.

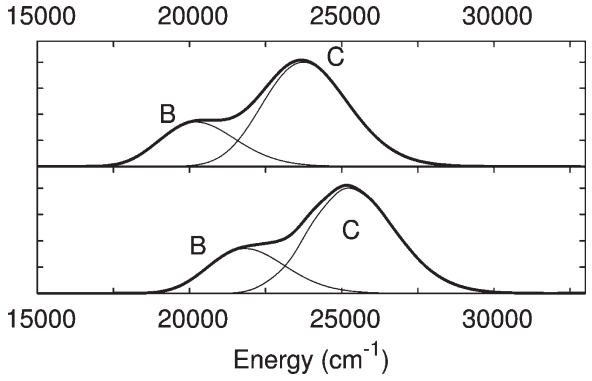

Figure 4. *T* = 0 K Br_2 (top) and $H_2O\cdots Br_2$ (bottom) $B(^3\Pi_{0_u^+}) \leftarrow X(^1\Sigma_g^+)$ and $C(^1\Pi_{1_u}) \leftarrow X(^1\Sigma_g^+)$ absorption spectra determined by wave packet propagation using ab initio potentials with spin−orbit correction for the *B* and *C* states. The thin curves represent the individual $B \leftarrow X$ and $C \leftarrow X$ components and the broad curves the overall absorption spectra.

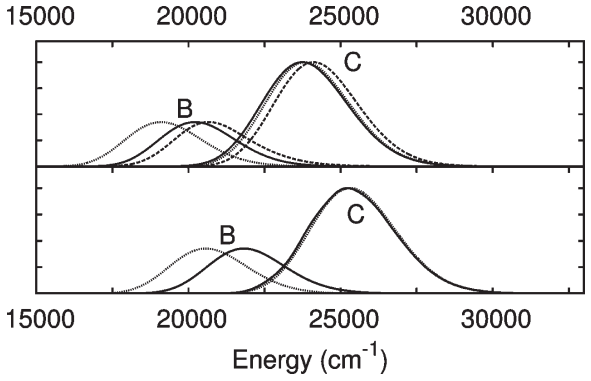

Figure 5. *T* = 0 K Br_2 (top) and $H_2O\cdots Br_2$ (bottom) $B(^3\Pi_{0_u^+}) \leftarrow X(^1\Sigma_g^+)$ and $C(^1\Pi_{1_u}) \leftarrow X(^1\Sigma_g^+)$ components of the absorption spectra calculated with the wave packet propagation method using the ab initio potentials including (straight lines) or not (dotted lines) spin−orbit correction, and empirical potentials from refs [21−25] (dashed lines).

effects are more important for the calculated vibrational frequency, which is 8 cm^{-1} smaller than the gas phase value, but the calculated change in $\hbar\omega_r$ upon dimer formation is within experimental error of the measured change in an Ar matrix. The calculated weak bond stretching frequency $\hbar\omega_R$ is 105 cm^{-1}. This is in satisfactory agreement with the experimental estimate that is obtained from the measured centrifugal distortion constant using the assumption of rigid monomers.

C. $H_2O\cdots Br_2$ Absorption Spectra. Figure 4 shows the *T* = 0 K Br_2 and $H_2O\cdots Br_2$ absorption spectra using wave packet propagation. Both the *B* and the *C* states contribute to the absorption. Because both states are repulsive in the Franck−Condon region (even though the *B* state has a well, vertical absorption accesses its repulsive wall), both spectra are broad and structureless, with the *B* spectrum being at lower energy. Upon complexation with water, the spectrum is strongly shifted to the blue. Somewhat surprisingly, adding the H_2O to the Br_2 chromophore has a minimal effect on the shape of the spectra. This will be discussed below.

In Figure 5, we compare the free Br_2 spectra calculated with and without spin−orbit coupling to those calculated with the empirical potentials. The long-range effects have the more important influence on the calculated spectra. Each band calculated from ab initio potential curves occur about 400 cm^{-1} to the red of those calculated from the empirical curves. This may be because the r_0 value is slightly too long, so that Franck−Condon excitation accesses lower energies in the excited states. The effect of spin−orbit on the sepctra is discussed in more details in section IIID.

1. Spectral Shifts. Values for the blue shifts upon interaction with water calculated for the dimer at several levels of approximation and measured for several experimental conditions are given in Table 3. The calculated shift due to complex formation with H_2O for the Br_2 $B \leftarrow X$ and $C \leftarrow X$ bands are about 1600 and 1500 cm^{-1}, respectively. The effect of spin−orbit is greatest for the $C \leftarrow X$ band, reducing its shift by almost 200 cm^{-1}.

The most important contribution to the shifts is due to bond formation in the ground electronic state. The calculated dimer zero-point energy is E_0 = −966.2632 cm^{-1}, and the calculated zero-point energy for Br_2 is 158.4209 cm^{-1}. Hence, the Br_2 v = 0 level is lowered by 1 125 cm^{-1} under complexation with water, which represents a contribution of ∼3/4 to the overall shift for *T* = 0 K, as was the case for $H_2O\cdots Cl_2$.[18] The rest of the shift comes from dimer repulsion in the excited states. Increasing the temperature decreases the shift because some of the intensity originates in vibrationally excited ground electronic levels. Ground electronic state vibrational excitation does not substantially change the net repulsion in the excited states after photoabsorption.

As can be seen from Table 3, the spectator model approximation gives a very good estimation of the spectral shifts. This is very

dx.doi.org/10.1021/jp110389z |*J. Phys. Chem. A* 2011, 115, 5983–5991

Table 3. Maxima for Br_2 and Maxima and Shifts (cm^{-1}) for $H_2O\cdots Br_2$ in the $C \leftarrow X$ and $B \leftarrow X$ Absorption Spectra, Compared to Experimental Measurements for Br_2 in Different Water Environments

	$C \leftarrow X$			$B \leftarrow X$		
	Br_2	$H_2O\cdots Br_2$		Br_2	$H_2O\cdots Br_2$	
environment	abs. max.	abs. max.	shift	abs. max.	abs. max.	shift
Br_2 gas, experiment, T = 293 K[a]	24270			20830		
wave packet calcd, T = 0 K, empirical[b]	24113			20667		
full wave packet calcd, T = 0 K[c]	23740	25221	1481	20214	21823	1611
full wave packet calcd, T = 120 K[c]	23728	25217	1489	20247	21795	1548
full wave packet calcd, T = 300 K[c]	23768	25140	1372	20267	21691	1424
wave packet calcd without S.O. correction[d]	23684	25325	1641	18952	20574	1622
spectator[e] model without S.O. correction[d]		25340	1660		20530	1580
vertical ab initio[f]			1916			1877
bromine hydrate clathrate, T = 250 K[a,g]		25150	880		21720	890
THF clathrate, T = 250 K [a,h]		24630	360		21190	360
CS-II bromine hydrate clathrate, T = 268 K[i]		24710	440		21270	440
aqueous solution (T = 293 K)[a]		26000	1730		22590	1760
amorphous ice (T = 120 K)[a]		25980	1710		22670	1640

[a] Ref 3. [b] Calculated using the empirically determined Br_2 potential energy curves.[21−25] [c] Calculated using the ab initio potential energy curves including the spin−orbit interactions in the B and C states. [d] Calculated using the ab initio curves without the spin−orbit correction. [e] See spectator model in ref 18. [f] Ref 18. [g] Values determined for the pure bromine hydrate-clathrate, TS-I structure, for which 80% of the bromine is trapped into $5^{12}6^2$ cages. [h] In this case, bromine was doped into the $5^{12}6^4$ cages of THF hydrate-clathrate. [i] These values, from ref 5, are for a newly observed bromine hydrate crystal in which the bromine is trapped in $5^{12}6^4$ cages.

Table 4. Calculated Full Widths at Half Maximum (FWHM, in cm^{-1}) for the $H_2O\cdots Br_2$ Complex $C \leftarrow X$ and $B \leftarrow X$ Absorption Spectra, Compared to the Br_2 Spectral Widths in the Gas Phase and in Different Water Environments

	$C \leftarrow X$		$B \leftarrow X$	
	Br_2	$H_2O\cdots Br_2$	Br_2	$H_2O\cdots Br_2$
gas phase, experimental[a]	3900		3650	
wave packet calcd, empirical, T = 0 K[b]	3209		2911	
full wave packet calcd, T = 0 K[c]	3293	3318	2922	2966
full wave packet calcd, T = 120 K[c]	3365	3451	3005	3132
Full wave packet calcd, T = 300K[c]	4106	4138	3672	3788
wave packet calcd without S.O. correction[d]	3241	3287	2932	2956
spectator[e] model without S.O. correction[d]		3172		2819
bromine hydrate clathrate, T = 250 K [a,f]		4000		3700
THF clathrate, T = 250 K [a,g]		4000		3700
aqueous solution (T = 293 K)[a]		5000		5000
amorphous ice (T = 120 K)[a]		4600		4300

[a] Ref 3. [b] Calculated using the empirically determined Br_2 potential energy curves.[21−25] [c] Calculated using the ab initio potential energy curves including the spin−orbit interactions in the B and C states. [d] Calculated using the ab initio curves without the spin−orbit correction. [e] See spectator model in ref 18. [f] Values determined for the pure bromine hydrate-clathrate, TS-I structure, for which 80% of the bromine is trapped. [g] In this case, bromine was doped into the $5^{12}6^4$ cages of THF hydrate-clathrate.

promising for predicting Br_2 spectra in more complex water environments. The vertical shift approximation (where the spectral shift is calculated as the difference between the $H_2O\cdots Br_2$ and Br_2 potential energy differences) overestimated the shift,[10] but the essential features are the same: most of the shift is due to the strong binding in the ground electronic state, 1182 cm^{-1}, the remaining ($\sim$700 cm^{-1}) being due to repulsion in the excited states.

2. Spectral Widths. The calculated widths for the two bands for each approximation, along with experimental widths for several environments, are collected in Table 4. Again, it is very satisfying that the ab initio results for free Br_2 agree so well with those calculated from empirical curves. For the T = 0 K spectra, the widths are narrow enough that the B-state shoulder on the red side of the band is clearly distinguishable and its position could be accurately determined from T = 0 K absorption spectra for both the free bromine molecule and the dimer formed with a water molecule.

As previously reported for $H_2O\cdots Cl_2$, dimer formation makes a surprisingly small contribution to the bandwidths for

dx.doi.org/10.1021/jp110389z |J. Phys. Chem. A 2011, 115, 5983–5991

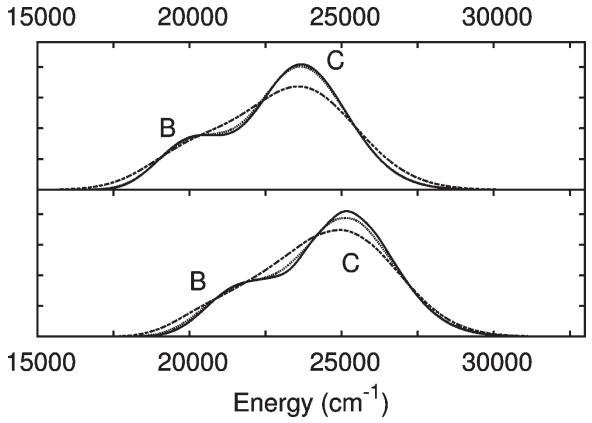

Figure 6. Comparison of the $T = 0$ K (straight lines), $T = 120$ K (dotted lines), and $T = 300$ K (dashed lines) Br_2 (top) and $H_2O\cdots Br_2$ (bottom) overall valence band absorption spectra, obtained with the wave packet propagation using ab initio potentials including the spin−orbit correction.

$H_2O\cdots Br_2$. Normally, one would expect the band widths to be a convolution of the Franck−Condon envelopes along the two active coordinates. That this in not the case here is due mainly to two effects. First, for most of the Franck−Condon excitation region the slope of the potential along R is quite small so that the reflection of the Franck−Condon envelope in energy for this coordinate would be narrow. Second, the effect of the dimer formation is to lower the slope of the repulsive wall along the Br−Br coordinate in the Franck−Condon region. So, the energy reflection of the Franck−Condon envelope for the r coordinate is narrower for the dimer than for the free molecule. This is why the spectator model gives a slightly smaller width than the free Br_2 width. The narrowing of the broadening in the r coordinate cancels the extra broadening due to the R coordinate upon complex formation.

D. Effect of the Spin−Orbit Coupling on the Br_2 and $H_2O\cdots Br_2$ Absorption Spectra. Figure 5 shows the effect of including spin−orbit terms on the absorption spectra of Br_2 and $H_2O\cdots Br_2$.

The inclusion of spin−orbit strongly shifts the position of the absorption maximum of the B state, as expected from the shift of the B potential energy. The resulting spectrum for Br_2 is in much better agreement with the $T = 0$ K spectrum obtained from empirical curves[21−25] fitted to the Br_2 spectrum at $T = 296$ to 713 K. However, this displacement is about the same ($\sim$1250 cm^{-1}) for Br_2 and $H_2O\cdots Br_2$, so there is no net change in the spectral shift. Surprisingly, the $C \leftarrow X$ band shift is more strongly affected by spin−orbit coupling. Although the C potential energy is displaced by only about 200 cm^{-1} for Br_2 in the Franck−Condon region, the spin−orbit correction calculated for the $C \leftarrow X$ $H_2O\cdots Br_2$ bandshift is 160 cm^{-1}. This is because the spin−orbit correction is more dependent on the H_2O-Br_2 interaction in the Franck−Condon region for the C state than for the B state, as was noted in section IIIA.

The width of the B state is not affected by spin−orbit coupling. This is another consequence of the fact that most of the width is governed by the r coordinate. Because the shift of the B state curve is almost constant with r in the Franck−Condon region, the width is unchanged by inclusion of spin−orbit effect. On the other hand, the slope of the C state is slightly steeper when spin−orbit coupling is included, which gives a slightly larger width (Table 4).

E. Effect of Temperature on the Spectra. Figure 6 shows the comparison of the spectra obtained at 0, 120, and 300 K. As expected, the spectra at 300 K are broader and red-shifted. The red shift is due to the superposition of spectra originating from higher vibrational levels and reaching more or less the same energy region in the excited states (the Franck−Condon region for an excited vibrational level is broader but not significantly displaced). The larger width for 300 K makes it more difficult to resolve the B from the C part of the spectrum, the B state now appearing only as a shoulder to the red. At $T = 120$ K, the spectra are already close to the ones at 0 K.

Even though the wave functions of the first excited vibrational levels have a larger amplitude in R, this does not affect their individual widths since they are controlled by the r coordinate. The overall broadening comes from the superposition of the $\upsilon_r = 1$ contribution, which has a larger amplitude in r and a larger width with an intensity node at the center (reflection principle).[26] This is superimposed with the contribution of all the populated excited vibrational levels in R, which originate from higher energy in the ground electronic state with no significant change in the energy accessed in the excited states.

Because the effect of the first, most strongly bonded solvent water molecule is already well described by a spectator model and makes a modest contribution to the bandwidths, we expect that homogeneous broadening will not be significant upon solvation of bromine in water. The simplest source of inhomogeneous broadening is vibrational excitation in the electronic ground state as the temperature increases. From the calculations presented here, $\sim$800 cm^{-1} of each Br_2 gas phase bandwidth at 300 K is due to thermal broadening. For the $H_2O\cdots Br_2$ dimer, this value is about the same. The bands in hydrate clathrate solid solutions are hardly broader than those of the gas phase, while those in aqueous solution exhibit an extra 1000 cm^{-1} of broadening. We suggest that this extra broadening is largely due to the fact that in aqueous solution the Br_2 molecules have a diverse range of success in competing with the surrounding water molecules to form halogen bonds. Hence the spectrum of each Br_2 molecule is shifted by a different amount (depending on its water environment) resulting in inhomogeneous spectral broadening.

For future experiments it is interesting to note that the distinct band separation for $T = 0$ K mostly survives to 120 K. If the spectra can be recorded for the clathrate hydrates at reduced temperatures it may be possible to observe the separate solvent effects on the two bands more effectively. This result also suggests that the broader widths observed for Br_2 in amorphous ice at 120 K[27] are due to inhomogeneous site effects rather than simple thermal broadening.

F. Comparison of Br_2 Spectra in Different Water Environments. It is quite remarkable that the calculated $H_2O\cdots Br_2$ shift is very comparable to the observed shift of Br_2 in water solution. In a previous publication,[18] we found that the calculated $H_2O\cdots Cl_2$ shift was much larger than the one observed for Cl_2 in liquid water. Indeed, the $H_2O\cdots Br_2$ shift is only 200 cm^{-1} smaller than that of Br_2 in aqueous solution, and much larger than in clathrate cages. The $H_2O\cdots Cl_2$ shift was 1 250 cm^{-1}, much larger than the 550 cm^{-1} shift measured in aqueous solution. A $H_2O\cdots X_2$ shift close to the one observed in water environment could reveal the presence of these binary complexes. This suggests that for bromine in aqueous solution, the bromine solvation shell contains water-halogen configurations with strong, linear halogen bonds while for chlorine the analogous bonding is not as effective. Indeed, a recent study[28] on

bromine aqueous solutions shows that bromine produces a strong perturbation on the liquid water structure. This difference could be due to the to the greater similarity of the Br−O bond energy to the water−water hydrogen bond energy. In this work we find that $D_0(H_2O\cdots Br_2)$ = 1124.684 cm^{-1} and $D_0(H_2O\cdots Cl_2)$ = 874.798 cm^{-1}, where $D_0(H_2O\cdots X_2)$ is the energy required to dissociate $H_2O\cdots X_2$ (v_r = 0, v_R = 0) to $H_2O + X_2(v = 0)$. For comparison, the water−water binding energy is $D_0(H_2O\cdots H_2O) = 1165 \pm 54$ cm^{-1} (refs 29 and 30). Hence, the $H_2O\cdots Br_2$ formation could compete with the $H_2O\cdots H_2O$ bonds around 300 K (200 cm^{-1}), but not $H_2O\cdots Cl_2$.

IV. CONCLUSIONS

We have presented spin−orbit corrected ab initio calculations of the valence electronic spectra of the $H_2O\cdots Br_2$ dimer using a 2-D model for the reduced dimensionality nuclear motion. The Br−Br and O−Br stretching motions are the minimum necessary to include the essential aspects of dimer formation on the spectra. Spin−orbit coupling is essential for obtaining the relative positions of the *B* and *C* state potential surfaces. Somewhat surprisingly, although spin−orbit coupling is most important for the *B* state, the spin−orbit influence on the band shift upon dimer formation is larger for the $C \leftarrow X$ band than for the $B \leftarrow X$ band. Another surprising result of this calculation is that the homogeneous broadening due to complex formation is minimal for the two valence excitation bands. This is attributed to the fact that the repulsive wall in the Br−Br stretching coordinate is somewhat less steep for the $H_2O\cdots Br_2$ dimer than for free Br_2. This effect cancels out most of the contribution to the broadening due to the repulsive wall along the O−Br stretching coordinate.

The magnitude of the calculated band shift upon dimer formation is 1610 cm^{-1} for the $B \leftarrow X$ band and 1481 cm^{-1} for the $C \leftarrow X$ band. These values are quite similar to the 1750 cm^{-1} band shift of the bromine valence spectrum upon aqueous solvation. This suggests that much of the aqueous solvation band shift can be attributed to the first nearest neighbor water molecule and that the effects of the other water molecules cancel out. It will be interesting to investigate whether this hypothesis survives higher dimensionality calculations and those that include more water molecules in the model. That the spectator model works so well to approximate the effects of the first nearest neighbor water molecule in the 2-D approximation suggests that it will provide a reasonable result for calculations including more water molecules and dynamical simulations of the nuclear motions. It also appears likely that the spectator model will be useful for exploring the hydrate-clathrate environment for which full dimensional calculations will be impossible for the foreseeable future.

The results presented here for $H_2O\cdots Br_2$ are similar to those presented previously for $H_2O\cdots Cl_2$. The calculated shift of the $H_2O\cdots Cl_2$ valence electronic spectra from that of free Cl_2 is also very important, 1250 cm^{-1}. In contrast, the observed valence spectrum band shift upon aqueous solvation is much smaller for Cl_2 than for Br_2. We hypothesize that this is due to the fact that the O−Br bond energy is more comparable to that of the water dimer bond energy, so that Br_2 competes more effectively for bonding with water than does Cl_2. Thus, the solvation shell of bromine in liquid water might contain water−halogen configurations with strong (linear) halogen bonds whereas chlorine does not.

Although the 2-D model presented here was the result of considerable effort due to the fact that including spin−orbit effects in the calculations is not trivial, we recognize that it will be important to investigate less approximate models in the future. Clearly, the effects of the wide amplitude bending motions will also be significant. One hopes that the spectator model will be useful for including these motions as well as adding more water molecules to the model.

AUTHOR INFORMATION

Corresponding Author

*E-mail: nadine.halberstadt@irsamc.ups-tlse.fr.

Present Addresses

[†]Laboratoire de Physique de l′ État Condensé, Université du Maine et CNRS (UMR 6087), Avenue Olivier Messiaen, F-72085 Le Mans cedex, France.

ACKNOWLEDGMENT

This work is dedicated to Victoria Buch, whose excellence, energy and enthusiasm for science inspired us. K.C.J. acknowledges support from the US-NSF Award Nos. CHE-0404743 and CHE-0911686. N.H., R.H.-L., M.I.B.U., and R.F.-M. acknowledge a CONACyT-CNRS collaboration grant (J110.320). N.H. and R.F.-M. would like to thank CNRS for a collaborative grant with K.C.J. (PICS 2009 No. 4648). Computer time has been provided by the laboratories of the authors.

REFERENCES

(1) Beckmann, E. Z. *Phys. Chem.* **1889**, *5*, 76.
(2) Gautier, C.; Charpy, M. *Comptes-Rendus de l'Académie des Sciences* **1890**, *110*, 189; **1890**, *111*, 645.
(3) Kerenskaya, G.; Goldschleger, I. U.; Apkarian, V. A.; Janda, K. C. *J. Phys. Chem. A* **2006**, *110*, 13792–13798.
(4) Goldschleger, I. U.; Kerenskaya, G.; Janda, K. C.; Apkarian, V. A. *J. Phys. Chem. A* **2008**, 787–789.
(5) Bernal-Uruchurtu, M. I.; Kerenskaya, G.; Janda, K. C. *Int. Rev. Phys. Chem.* **2009**, *28*, 223–265.
(6) Lowig, C. *Magn. Pharm.* **1828**, *23*, 12.
(7) Lowig, C. *Ann. Chim. Phys. Ser.* **1829**, *42*, 113–119.
(8) Udachin, K. A.; Enright, G. D.; Ratcliffe, C. I.; Ripmeester, J. A. *J. Am. Chem. Soc.* **1997**, *119*, 11481–11486.
(9) Schofield, D. P.; Jordan, K. D. *J. Phys. Chem. A* **2009**, *113*, 7431–7438.
(10) Hernández Lamoneda, R.; Uc Rosas, V. H.; Bernal Uruchurtu, M. I.; Halberstadt, N.; Janda, K. C. *J. Phys. Chem. A* **2008**, *112*, 89–96.
(11) Bernal-Uruchurtu, M. I.; Hernández-Lamoneda, R.; Janda, K. C. *J. Phys. Chem. A* **2009**, *113*, 5496–5505.
(12) Hernández Lamoneda, R.; Janda, K. C. *J. Chem. Phys.* **2005**, *123*, 161102.
(13) NIST Handbook of Basic Atomic Spectra, http://physics.nist.gov/PhysRefData/Handbook/Tables/chlorinetable5.htm.
(14) From NIST, $A_\gamma(X) = m(X)[m(12C)/12]$; $A_\gamma(^{16}O)$ = 15.99491461956(16); $A_r(H)$ = 1.00782503207(10); $A_r(^{79}Br)$ = 78.9183371(22); see URL http://physics.nist.gov/PhysRefData/ASD/levelsform.html.
(15) Dolg, M. *Ph.D. Thesis*, University of Stuttgart, Germany, 1989.
(16) Bergner, A.; Dolg, M.; Kuechle, W.; Stoll, H.; Preuss, H. *Mol. Phys.* **1993**, *80*, 1431.
(17) Amos, R.D.; et al. *MOLPRO*, a package of ab initio programs, version 2006.1; Werner, H.-J., Knowles, P. J., Eds., University College Cardiff Consultants Limited: Cardiff, UK, 2006.

(18) Franklin-Mergarejo, R.; Rubayo-Soneira, J.; Halberstadt, N.; Ayed, T.; Bernal Uruchurtu, M.; Hern′andez-Lamoneda, R.; Janda, K. C. *J. Phys. Chem. A* **2009**, *113*, 7563–7569.
(19) From NIST, see URL http://www.nist.gov/physlab/data/comp.cfm.
(20) Le Roy, R. J.; Macdonald, R. G.; Burns, G. *J. Chem. Phys.* **1976**, *65*, 1485–1500.
(21) Barrow, R. F.; Clark, T. C.; Coxon, J. A.; Lee, K. K. *J. Mol. Spectrosc.* **1974**, *51*, 428–438.
(22) Focsa, C.; Li, H.; Bernath, P. F. *J. Mol. Spectrosc.* **2000**, *200*, 104–119.
(23) Clyne, M. A.; Heaven, M. C.; Tellinghuisen, J. *J. Chem. Phys.* **1982**, *76*, 5341–5349.
(24) Tellinghuisen, J. *J. Chem. Phys.* **2001**, *115*, 10417–10424.
(25) Tellinghuisen, J. *J. Chem. Phys.* **2003**, *118*, 15731574.
(26) Schinke, R. *Photodissociation Dynamics*; Cambridge University Press: New York, 1995.
(27) Goldschleger, I. U.; Senekerimyan, V.; Krage, M. S.; Seferyan, H.; Janda, K. C.; Apkarian, V. A. *J. Chem. Phys.* **2006**, *124*, 204507.
(28) Bernal-Uruchurtu, M. I., private communication.
(29) Mas, E. M.; Bukowski, R.; Szalewicz, K.; Groenenboom, G. C.; Wormer, P. E. S.; van der Avoird, A. *J. Chem. Phys.* **2000**, *113*, 6687–6701.
(30) Curtiss, L. A.; Frurip, D. J.; Blander, M. *J. Chem. Phys.* **1979**, *71*, 2703–2711.
(31) Legon, A. C.; Thumwood, J. M.; Waclawik, E. R. *Chem.—Eur. J.* **2002**, *8*, 940–950.
(32) Engdahl, A.; Nelander, B. *J. Chem. Phys.* **1986**, *84*, 1981–1987.
(33) Langen, J.; Lodemann, K. P.; Schurath, U. *Chem. Phys.* **1987**, *112*, 393–408.